



Higher-dimensional topological dS black hole with a nonlinear source and its thermodynamics and phase transitions

Hai-Long Zhen^{1,2}, Yun-Zhi Du^{1,2}, Huai-Fan Li^{1,2}, Li-Chun Zhang^{1,2}, Yu-Bo Ma^{1,2,a}

¹ Department of Physics, Shanxi Datong University, Datong 037009, China

² Institute of Theoretical Physics, Shanxi Datong University, Datong 037009, China

Received: 15 April 2024 / Accepted: 25 June 2024

© The Author(s) 2024

Abstract In this paper, the higher-dimensional topological dS black hole with a nonlinear source (HDTNS) is considered. First, we obtain the thermodynamic quantities of the $(n+1)$ -dimensional topological dS black hole, which satisfy the first law of thermodynamics. Second, based on the effective thermodynamic quantities and Maxwell's equal-area law method, we explore the phase equilibrium for the HDTNS. The boundary of the two-phase coexistence region in the $P_{\text{eff}}^0 - T_{\text{eff}}^0$ diagram is obtained. The critical thermodynamic quantities as well as the horizon potential are also investigated. Furthermore, we analyze the effect of parameters (the spacetime dimension n and the ratio of two horizon radii $x = r_+/r_c$) on the boundary of the two-phase coexistence region and study the latent heat of phase transition for this system, which corresponds to the Clapeyron equation. The results indicate that the phase transition in HDTNS spacetime is analogous to that in a van der Waals (vdW) fluid system, which is determined by electrical potential at the horizon. These results help to understand the fundamental properties of black holes. A more intuitive and profound understanding of gravity is gained by studying the thermodynamic properties of different spacetimes. They provide a theoretical basis for an in-depth study of the classical and quantum properties of de Sitter spacetime and its evolution.

1 Introduction

As a thermodynamic system, the black hole is closely related to classical thermodynamics, gravitation, and quantum systems. The study of the thermodynamic properties and phase transitions of anti-de Sitter (AdS) black holes or dS spacetimes with black holes has received considerable attention [1–27]. Treating the cosmological constant Λ as a thermo-

dynamic pressure and its conjugate quantity as a thermodynamic volume established the first law of black hole thermodynamics in the extended phase space. This approach allowed for the investigation of the thermodynamic properties of AdS black holes. Notably, the thermodynamic properties of black holes in AdS space differ significantly from those of black holes in asymptotically flat spacetime or in de Sitter space. In AdS space, the phase transition can be explained through the AdS/conformal field theory (CFT) correspondence [28–30]. The phase transition of charged AdS black holes is quite similar to that of a van der Waals (vdW) system. Furthermore, black hole chemistry has revealed a broad range of new phenomena associated with black holes, such as triple points [31], reentrant phase transitions [32], and heat engines [33].

Astronomical observations indicate that the expansion of our universe is accelerating [34–36], suggesting that it will eventually become an asymptotic de Sitter universe. The study of the thermodynamics of asymptotic de Sitter black holes has been motivated by the formulation of the dS/CFT correspondence [30] and the physical relevance of de Sitter black holes in cosmology [37]. If we consider the cosmological constant as dark energy, our universe will eventually enter a new dS phase. Therefore, a clear understanding of dS spacetime is essential [38–40]. However, this subject is not well understood. In dS space, the absence of a Killing vector, which is time-like everywhere outside the black hole horizon, raises questions about the notion of asymptotic mass [38]. Additionally, the presence of both the black hole horizon and cosmological horizon, which have different temperatures, suggests that the system does not meet the requirements of thermodynamic equilibrium. The thermodynamic properties of dS spacetime are of direct interest to cosmology, but these features present unfortunate difficulties. There have been a few attempts to investigate the thermodynamics of black holes in dS spacetime and overcome this problem.

^a e-mail: yuboma.phy@gmail.com (corresponding author)

One way to deal with the thermodynamics of asymptotically dS black hole spacetimes is to first formulate several separate thermodynamic laws, one for each “physical” horizon present in the spacetime [41–43]. One way to approach this task is by using the concept of effective temperature [44–46]. This involves focusing on an observer situated in an “observable part of the universe,” located between the black hole horizon and the cosmological horizon. Another approach is to examine de Sitter black holes that are enclosed in an isothermal cavity at a fixed temperature. This fragment describes the definition of a grand canonical ensemble in which the cavity acts as a reservoir, allowing for the existence of thermodynamically stable black holes. Brown [47] first explored this approach, demonstrating the stability of the ensemble. Later, Carlip and Vaidya [48] found a Hawking–Page-like phase transition in both the asymptotically flat and de Sitter cases.

Nonlinear field theories are of interest to various branches of mathematical physics because most physical systems are inherently nonlinear. The main reason for considering nonlinear electrodynamics (NLED) is that these theories have considerably richer content than the Maxwell field, and in special cases, they reduce to the linear Maxwell theory. The authors in [49] presented $(n+1)$ -dimensional topological static black hole solutions of Einstein gravity in the presence of NLED. They checked the first law of thermodynamics and studied the stability of the solutions in both canonical and grand canonical ensembles [50,51]. Additionally, they analyzed the effect of the nonlinear charge correction on the thermodynamic properties of the black hole [52–56]. A natural question that arises is whether a dS spacetime with a nonlinear charge source has thermodynamic properties similar to an AdS black hole. In this work, the higher-dimensional dS spacetime with the nonlinear charge correction is considered an ordinary thermodynamic system by examining the correlation between two horizons. The focus is on investigating the thermodynamics and phase transitions of the $(n+1)$ -dimensional dS spacetime. The analysis also considers the effect of nonlinear charge correction on the phase transition. The results show that the latent heat of phase transition and the two-phase coexistence region are similar to those of an ordinary thermodynamic system.

The remainder of this paper is organized as follows: In Sect. 2, we briefly present the thermodynamic quantities in HDTNS and establish the state equation of HDTNS which corresponds to the ordinary thermodynamic system [57–60]. Then the $P_{\text{eff}}^0 - T_{\text{eff}}^0$ curves, the phase diagrams in $P_{\text{eff}}^0 - V$, and the $\frac{q^2}{r^{2n-4}} - x(y)$ curves in HDTNS are presented. The effects of the ratio x between two horizons and the spacetime dimensions n on them are discussed in Sect. 3. The slope of the $P_{\text{eff}}^0 - T_{\text{eff}}^0$ curve for different spacetime dimensions n is given, which corresponds to the Clapeyron equation. The

latent heat of the phase transition for the first-order phase transition in HDTNS and the effect of the ratio x between two horizons and the spacetime dimensions n on it are given in Sect. 4. Finally, a brief summary is given in Sect. 5.

2 Topological black hole with nonlinear source

The $(n+1)$ -dimensional action of Einstein gravity with nonlinear electrodynamics is [49–51,61]:

$$I_G = -\frac{1}{16\pi} \int_{\mathcal{M}} d^{n+1}x \sqrt{-g} [R - 2\Lambda + L(\mathcal{F})] - \frac{1}{8\pi} \int_{\partial\mathcal{M}} d^n x \sqrt{-\gamma} \Theta(\gamma), \quad (2.1)$$

where R is the scalar curvature and Λ is the cosmological constant. In this action,

$$L(\mathcal{F}) = -\mathcal{F} + \alpha \mathcal{F}^2 + \mathcal{O}(\alpha^2), \quad (2.2)$$

is the Lagrangian of nonlinear electrodynamics. $\mathcal{F} = F_{\mu\nu} F^{\mu\nu}$ is the Maxwell invariant, in which $F_{\mu\nu} = \partial_\mu A_\nu - \partial_\nu A_\mu$ is the electromagnetic field tensor and A_μ is the gauge potential. In addition, α denotes the nonlinearity parameter, which is small, so the effects of nonlinearity should be considered as a perturbation. In the second integral, γ and Θ are, respectively, the trace of induced metric, $\gamma_{i,j}$, and the extrinsic curvature $\Theta_{i,j}$ on the boundary $\partial\mathcal{M}$. The variation of the action (2.1) with respect to the metric tensor $g_{\mu\nu}$ and the Faraday tensor $F_{\mu\nu}$ leads to

$$G_{\mu\nu} + \Lambda g_{\mu\nu} = \frac{1}{2} g_{\mu\nu} L(\mathcal{F}) - 2L_{\mathcal{F}} F_{\mu\lambda} F_\nu^\lambda, \quad (2.3)$$

$$\partial_\mu (\sqrt{-g} L_{\mathcal{F}} F^{\mu\nu}) = 0, \quad (2.4)$$

where $G_{\mu\nu}$ is the Einstein tensor and $L_{\mathcal{F}} = dL(\mathcal{F})/d\mathcal{F}$.

The $(n+1)$ -dimensional topological black hole solutions can take the form of

$$ds^2 = -f(r)dt^2 + \frac{dr^2}{f(r)} + r^2 d\Omega_{n-1}^2, \quad (2.5)$$

where

$$f(r) = k - \frac{m}{r^{n-2}} - \frac{2\Lambda r^2}{n(n-1)} + \frac{2q^2}{(n-1)(n-2)r^{2n-4}} - \frac{4q^4\alpha}{(3n^7 - 7n + 4)r^{2n-6}}, \quad (2.6)$$

m is an integration constant which is related to the mass of the black hole, and the last term in Eq. (2.6) indicates the effect of nonlinearity. The asymptotic behavior of the solution is

AdS or dS provided $\Lambda < 0$ or $\Lambda > 0$, and the case of the asymptotically flat solution is permitted for $\Lambda = 0$ and $k = 1$.

When $\Lambda > 0$, the black hole horizon r_+ and the cosmological horizon r_c exist in spacetime, and the position of two horizons satisfies the equation $f(r_{+,c}) = 0$. The radiation temperature of the two horizons is given by

$$T_+ = \frac{f'(r_+)}{4\pi} = \frac{1}{2\pi(n-1)} \times \left(\frac{(n-1)(n-2)k}{2r_+} - \Lambda r_+ - \frac{q^2}{r_+^{2n-3}} + \frac{2q^4\alpha}{r_+^{4n-5}} \right). \quad (2.7)$$

$$T_c = -\frac{f'(r_c)}{4\pi} = -\frac{1}{2\pi(n-1)} \times \left(\frac{(n-1)(n-2)k}{2r_c} - \Lambda r_c - \frac{q^2}{r_c^{2n-3}} + \frac{2q^4\alpha}{r_c^{4n-5}} \right). \quad (2.8)$$

The mass of the black hole

$$M = \frac{V_{n-1}(n-1)}{16\pi} \times \left(kr_+^{n-2} - \frac{2\Lambda r_+^n}{n(n-1)} + \frac{2q^2}{(n-1)(n-2)r_+^{n-2}} - \frac{4q^4\alpha}{[2(n-2)(n+2)+(n-3)(n-4)]r_+^{3n-4}} \right)$$

or

$$M = \frac{V_{n-1}(n-1)}{16\pi} \times \left(kr_c^{n-2} - \frac{2\Lambda r_c^n}{n(n-1)} + \frac{2q^2}{(n-1)(n-2)r_c^{n-2}} - \frac{4q^4\alpha}{[2(n-2)(n+2)+(n-3)(n-4)]r_c^{3n-4}} \right). \quad (2.9)$$

$$\begin{aligned} V_{n-1} &= \frac{2\pi^{n/2}}{\Gamma(n/2)}, \quad S_{+,c} = \frac{V_{n-1}r_{+,c}^{n-1}}{4}, \\ V_{+,c} &= \frac{V_{n-1}r_{+,c}^n}{n}, \quad Q = \frac{q}{4\pi}V_{n-1}, \\ \Phi_{+,c} &= \frac{q}{(n-2)r_{+,c}^{n-2}} - \frac{4q^3\alpha}{(3n-4)r_{+,c}^{3n-4}}, \\ P &= -\frac{\Lambda}{8\pi}, \quad M = \frac{V_{n-1}(n-1)m}{16\pi}. \end{aligned} \quad (2.10)$$

Thermodynamic quantities corresponding to two horizons satisfy the first law of thermodynamics

$$dM = T_{+,c}dS_{+,c} + \Phi_{+,c}dQ + V_{+,c}dP. \quad (2.11)$$

Treating the spacetime of HDTNS, which includes the horizons of both black holes and cosmology, as a thermodynamic system, it must adhere to the universal first law of thermodynamics according to Eq. (2.11). [27]

$$dM = T_{\text{eff}}dS + P_{\text{eff}}dV + \Phi_{\text{eff}}dQ, \quad (2.12)$$

Here, the thermodynamic volume is that between the black hole horizon and the cosmological horizon, namely [38]

$$V = V_c - V_+ = \frac{V_{n-1}r_c^n}{n}(1-x^n). \quad (2.13)$$

Taking the dimension into account, we set the entropy of the spacetime as follows

$$S = \frac{V_{n-1}r_c^{n-1}}{4}F_n(x). \quad (2.14)$$

with $F_n(x)$ as a function of x , where $x = r_+/r_c$ denotes the position ratio between the black hole horizon r_+ and the cosmological horizon r_c , and the effective temperature T_{eff} , the effective pressure P_{eff} , and the effective potential Q_{eff} of the system are determined from Eq. (2.12), respectively

$$T_{\text{eff}} = \frac{f_1(x)}{r_c} + \frac{q^2f_2(x)}{r_c^{2n-3}} - \frac{4q^4\alpha f_3(x)}{r_c^{4n-5}}, \quad (2.15)$$

with

$$\begin{aligned} f_1(x) &= \frac{k((n-2-nx^2)(1-x^n)+2(n-1)x^n(1-x^2))}{4\pi x(1+x^{n+1})}, \\ f_2(x) &= \frac{nx^n(1-x^{n-2})-(n-2)(1-x^{3n-2})}{2\pi x^{2n-3}(1+x^{n+1})(n-1)(n-2)}, \\ f_3(x) &= \frac{-(3n-4)+(3n-4)x^{5n-4}+nx^n(1-x^{3n-4})}{\pi(1+x^{n+1})(3n-4)(n-1)x^{4n-5}}, \\ F_n(x) &= \frac{3n-1}{2n-1}(1-x^n)^{(n-1)/n} - \frac{n(1+x^{2n-1})-(2n-1)x^{n-1}(1+x)}{(2n-1)(1-x^n)}. \end{aligned} \quad (2.16)$$

$$\begin{aligned} \Phi_{\text{eff}} &= \left(\frac{\partial M}{\partial Q} \right)_{S,V} \\ &= \frac{(n-1)(1-x^{2n-2})q}{(1-x^n)r_c^{n-2}x^{n-2}} \left[\frac{1}{(n-1)(n-2)} \right. \\ &\quad \left. - \frac{4q^2\alpha}{(3n^2-7n+4)r_c^{2n-2}} \frac{(1+x^{2n-2})}{x^{2n-2}} \right]. \end{aligned} \quad (2.17)$$

$$P_{\text{eff}} = \frac{f_4(x)}{r_c^2} + \frac{q^2f_5(x)}{r_c^{2n-2}} - \frac{q^4\alpha f_6(x)}{r_c^{4n-4}} \quad (2.18)$$

with

$$\begin{aligned}
f_4(x) &= \frac{-k}{16\pi(1+x^{n+1})} \left(\frac{F_n(x)(n-1)(n-2-nx^2+2x^n)}{x(1-x^n)} - F'_n(x)(1-x^2)(n-2) \right) \\
f_5(x) &= \frac{-1}{8\pi x^{2n-3}(n-1)(1+x^{n+1})} \left(\frac{F_n(x)(n-1)[2(n-1)x^n-(n-2)-nx^{2n-2}]}{(n-2)(1-x^n)} + xF'_n(x)(1-x^{2n-2}) \right) \\
f_6(x) &= -\frac{F_n(x)(n-1)[(3n-4)+4(n-1)x^n-nx^{4n-4}]+xF'_n(x)(3n-4)(1-x^n)(1-x^{4n-4})}{4\pi x^{4n-5}(1+x^{n+1})(1-x^n)(3n-4)(n-1)}. \tag{2.19}
\end{aligned}$$

substituting Eq. (2.15) into Eq. (2.18), one obtain

$$\begin{aligned}
P_{\text{eff}} &= \frac{f_6(x)T_{\text{eff}}}{r_c f_3(x)} - \frac{f_1(x)f_6(x) - f_4(x)f_3(x)}{r_c^2 f_3(x)} \\
&+ \frac{q^2(f_5(x)f_3(x) - f_2(x)f_6(x))}{r_c^{2n-2} f_3(x)}. \tag{2.20}
\end{aligned}$$

The thermodynamic quantities presented above are obtained by treating the whole HDTNS spacetime as a thermodynamic system. Therefore, this approach enables us to obtain thermodynamic quantities that reflect the thermodynamic properties of the HDTNS spacetime. Based on this analysis, the thermodynamic properties of the HDTNS spacetime can be evaluated.

3 The construction of the equal-area law in the $P - V$ diagram

When the ratio x of the two horizons in the HDTNS spacetime is constant, the effective temperature is T_{eff}^0 ($T_{\text{eff}}^0 \leq T_{\text{eff}}^c$), and T_{eff}^c is the critical temperature. For the system to satisfy the thermodynamic equilibrium condition, the horizontal coordinates of the boundaries of the two-phase coexistence region in the HDTNS spacetime must be V_2 and V_1 , respectively, and the vertical coordinate of the pressure is P_{eff}^0 . The value of P_{eff}^0 is determined by the cosmological horizon radius r_c . By Maxwell's equal-area law [27, 57, 58, 60]

$$P_{\text{eff}}^0(V_2 - V_1) = \int_{V_1}^{V_2} P_{\text{eff}} \, dV, \tag{3.1}$$

through Eq. (3.1), we obtain

$$\begin{aligned}
P_{\text{eff}}^0 &= \frac{f_6(x)T_{\text{eff}}^0}{r_1 f_3(x)} - \frac{f_1(x)f_6(x) - f_4(x)f_3(x)}{r_1 f_3(x)} \\
&+ \frac{q^2(f_5(x)f_3(x) - f_2(x)f_6(x))}{r_1^{2n-2} f_3(x)}
\end{aligned}$$

$$\begin{aligned}
P_{\text{eff}}^0 &= \frac{f_6(x)T_{\text{eff}}^0}{r_2 f_3(x)} - \frac{f_1(x)f_6(x) - f_4(x)f_3(x)}{r_2 f_3(x)} \\
&+ \frac{q^2(f_5(x)f_3(x) - f_2(x)f_6(x))}{r_2^{2n-2} f_3(x)}, \tag{3.2}
\end{aligned}$$

where r_2 and r_1 stand for the positions of the cosmological horizons of two regions of phase coexistence, respectively.

$$\begin{aligned}
P_{\text{eff}}^0 \frac{r_2^n}{n} (1 - y^n) &= \frac{T_{\text{eff}}^0 f_6(x) r_2^{n-1} (1 - y^{n-1})}{(n-1) f_3(x)} \\
&- \frac{[f_1(x)f_6(x) - f_4(x)f_3(x)] r_2^{n-2} (1 - y^{n-2})}{(n-2) f_3(x)} \\
&+ \frac{q^2(f_2(x)f_6(x) - f_5(x)f_3(x)) (1 - y^{n-2})}{(n-2) r_2^{n-2} y^{n-2} f_3(x)}. \tag{3.3}
\end{aligned}$$

Through Eq. (3.2), we obtain

$$\begin{aligned}
0 &= -f_6(x)T_{\text{eff}}^0(1-y) \\
&+ \frac{(f_1(x)f_6(x) - f_4(x)f_3(x))(1-y^2)}{r_2 y} \\
&- \frac{q^2(f_5(x)f_3(x) - f_2(x)f_6(x))(1-y^{2n-2})}{r_2^{2n-3} y^{2n-3}}, \tag{3.4}
\end{aligned}$$

$$\begin{aligned}
P_{\text{eff}}^0 &= \frac{f_6(x)T_{\text{eff}}^0(1+y)}{2r_2 y f_3(x)} \\
&- \frac{(f_1(x)f_6(x) - f_4(x)f_3(x))(1+y^2)}{2r_2^2 y^2 f_3(x)} \\
&+ \frac{q^2(f_5(x)f_3(x) - f_2(x)f_6(x))(1+y^{2n-2})}{2r_2^{2n-2} y^{2n-2} f_3(x)}. \tag{3.5}
\end{aligned}$$

where $y = r_1/r_2$ is the cosmological (black hole) horizon position ratio of the two-phase coexistence region. Through Eqs. (3.3) and (3.5), we obtain

$$\begin{aligned}
& \frac{f_6(x)T_{\text{eff}}^0[(1+y)(1-y^n)-n(1-y)(1+y^n)]}{2(n-1)} \\
& + \frac{(f_1(x)f_6(x)-f_4(x)f_3(x))[(n-2)(1-y^{n+2})-(n+2)y^2(1-y^{n-2})]}{2r_2y(n-2)} \\
& = \frac{q^2(f_5(x)f_3(x)-f_2(x)f_6(x))[(n-2)(1+y^{2n-2})(1-y^n)-2ny^n(1-y^{n-2})]}{2r_2^{2n-3}y^{2n-3}(n-2)}. \tag{3.6}
\end{aligned}$$

Through Eqs. (3.4) and (3.6), we obtain

$$\frac{q^2}{r_2^{2n-4}y^{2n-4}} = \frac{f_1(n, y)[f_1(x)f_6(x)-f_4(x)f_3(x)]}{f_2(n, y)[f_5(x)f_3(x)-f_2(x)f_6(x)]}, \tag{3.7}$$

with

$$\begin{aligned}
f_1(n, y) &= \left[\frac{(1+y)[(1+y)(1-y^n)-n(1-y)(1+y^n)]}{(n-1)} + \frac{[(n-2)(1-y^{n+2})-(n+2)y^2(1-y^{n-2})]}{(n-2)} \right] \\
f_2(n, y) &= \left[\frac{[(n-2)(1+y^{2n-2})(1-y^n)-2ny^n(1-y^{n-2})]}{(n-2)} + \frac{(1-y^{2n-2})[(1+y)(1-y^n)-n(1-y)(1+y^n)]}{(n-1)(1-y)} \right]
\end{aligned}$$

From Eq. (3.2), we obtain

$$\begin{aligned}
P_{\text{eff}}^0 &= \frac{f_1(x)f_6(x)-f_4(x)f_3(x)}{r_2^2yf_3(x)} \\
&\times \left(1 - \frac{(1-y^{2n-3})}{(1-y)} \frac{f_1(n, y)}{f_2(n, y)} \right) \tag{3.8}
\end{aligned}$$

$$\begin{aligned}
T_{\text{eff}}^0 &= \frac{f_1(x)f_6(x)-f_4(x)f_3(x)}{r_2yf_6(x)} \\
&\times \left((1+y) - \frac{(1-y^{2n-2})}{(1-y)} \frac{f_1(n, y)}{f_2(n, y)} \right) \tag{3.9}
\end{aligned}$$

Combining Eqs. (3.8) and (3.9), the $P_{\text{eff}}^0 - T_{\text{eff}}^0$ curve for the two-phase equilibrium coexistence is shown in Fig. 1.

From Fig. 1, the effective transition temperature T_{eff}^0 and pressure P_{eff}^0 of the two-phase coexistence are affected by the spacetime dimension n and the ratio x when the phase transition occurs in the HDTNS spacetime. As shown in Fig. 1a, the position of the critical point in HDTNS spacetime increases with increasing x , the critical temperature T_{eff}^c and the pressure P_{eff}^c (the endpoint of the curve) increase with n , and the behavior of the effective transition pressure P_{eff}^0 decreases with increasing n for a given effective transition temperature T_{eff}^0 . Figure 1b shows that the behavior of the critical temperature T_{eff}^c in HDTNS spacetime decreases with the increase in the value of x . However, the behavior of the critical pressure P_{eff}^c in HDTNS spacetime increases with the increasing

value of x . The behavior of the effective transition pressure P_{eff}^0 increases with the increasing value of x for a given effective transition temperature T_{eff}^0 .

When $y \rightarrow 1$, by Eq. (3.7), the position of the critical point of the cosmological horizon, r_{cc} , for different dimensions n in HDTNS spacetime satisfies

$$r_{cc}^{2n-4} = \frac{q^2(n-1)(2n-3)(f_5(x)f_3(x)-f_2(x)f_6(x))}{f_1(x)f_6(x)-f_4(x)f_3(x)}. \tag{3.10}$$

The critical temperature T_{eff}^c and the critical pressure P_{eff}^c satisfy the following equation

$$\begin{aligned}
T_{\text{eff}}^c &= \frac{4(n-2)[f_1(x)f_6(x)-f_4(x)f_3(x)]}{(2n-3)f_6(x)r_{cc}} \\
&= \frac{4(n-2)[f_1(x)f_6(x)-f_4(x)f_3(x)]}{(2n-3)f_6(x)} \\
&\times \left(\frac{f_1(x)f_6(x)-f_4(x)f_3(x)}{q^2(n-1)(2n-3)(f_5(x)f_3(x)-f_2(x)f_6(x))} \right)^{1/(2n-4)}, \\
P_{\text{eff}}^c &= \frac{(n-2)(f_1(x)f_6(x)-f_4(x)f_3(x))}{(n-1)f_3(x)r_{cc}^2}. \tag{3.11}
\end{aligned}$$

The values of x in Eqs. (3.10) and (3.11) can take on any value of $0 < x < 1$. However, for a thermodynamic system, these values must satisfy $r_{cc} > 0$, $P_{\text{eff}}^c > 0$, $T_{\text{eff}}^c > 0$. The critical values for the reaction in Fig. 2 vary depending on the value of x .

Figure 2 shows the critical horizon position r_{cc} , the critical temperature T_{eff}^c , and the critical pressure P_{eff}^c of spacetime for a fixed x increase with increasing spacetime dimension n .

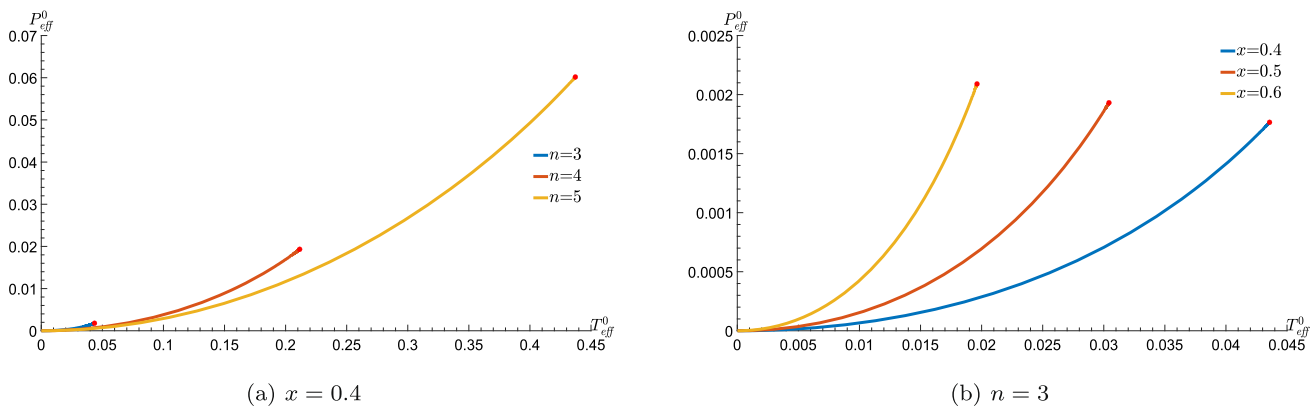


Fig. 1 The $P_{\text{eff}}^0 - T_{\text{eff}}^0$ curve in two-phase equilibrium coexistence (setting $q = 1$)

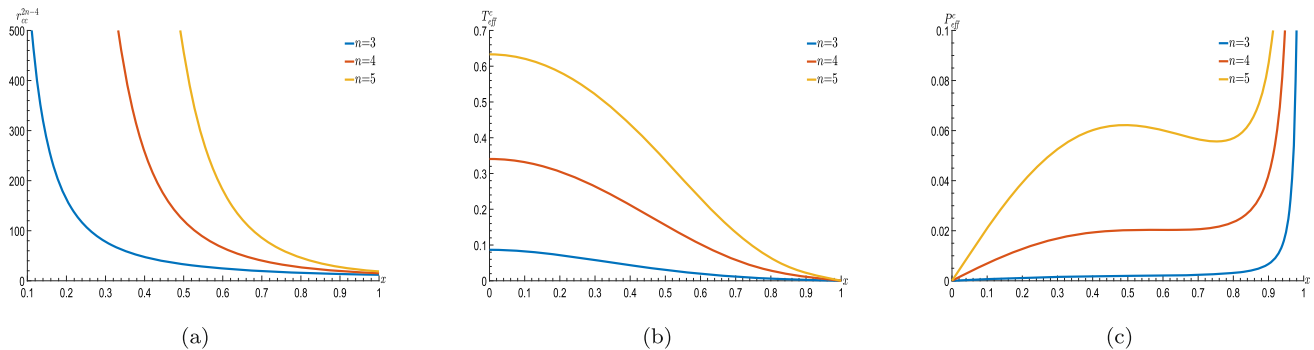


Fig. 2 The behavior of r_{cc}^{2n-4} , T_{eff}^c , and P_{eff}^c as a function of x (setting $q = 1$)

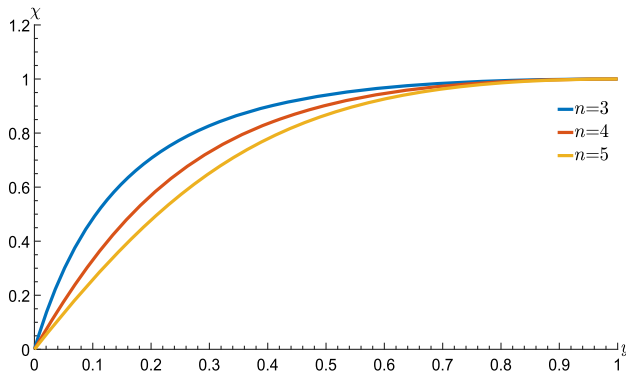


Fig. 3 The behavior of χ as a function of y

Taking $T_{\text{eff}}^0 = \chi T_{\text{eff}}^c$, from Eqs. (3.9) and (3.11) we obtain

$$\chi = \frac{(2n-3)}{4(n-2)(1-y)} \left(\frac{(n-1)(2n-3)f_1(n, y)}{f_2(n, y)} \right)^{1/(2n-4)} \times \left[(1-y^2) - \frac{(1-y^{2n-2})f_1(n, y)}{f_2(n, y)} \right]. \quad (3.12)$$

Figure 3 shows the change in the effective temperature T_{eff} of spacetime as a function of the cosmological (or the black hole) horizon position ratio y of the two-phase coexistence

region during a first-order phase transition. Figure 3 shows that the effective temperature T_{eff}^0 of the coexistence region for a fixed y decreases with increasing spacetime dimension n .

Because of the existence of gravity in the system, the interplay between the black hole and cosmology horizons should be considered, and we say that the thermodynamic volume is that between the black hole horizon and the cosmological horizon, $V = V_c - V_+$, i.e., Eq. (2.13) in this work. On the other hand, for the space between the black hole outer horizon (generally called the black hole horizon) and cosmology horizon, the different Hawking temperatures on the two horizons prevent a dS spacetime with a black hole in equilibrium as similar to an ordinary thermodynamic system, while there are common parameters M, Q on the black hole and cosmological horizons. Thus, the thermodynamic quantities on the two horizons are not independent. The interplay between the two horizons must be taken into account when constructing the effective quantities of a dS spacetime with a black hole in thermodynamic equilibrium. From $V_{+,c}$ in Eq. (2.10) and the definition $x = r_+/r_c$, the relationship of the effective pressure P_{eff} and the ratio x is established. Based on these and Ehrenfest's classification of phase transitions, the system undergoes a phase transition that satisfies the conditions for a

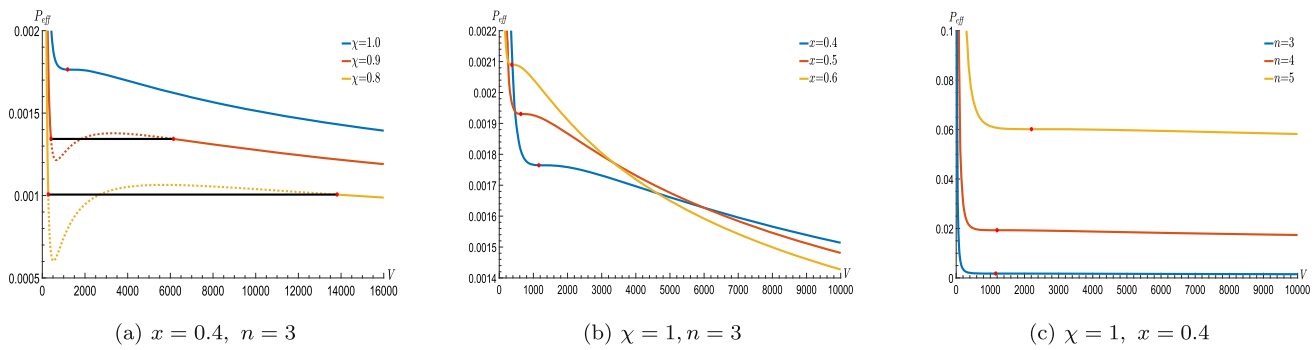


Fig. 4 The behavior of the effective pressure P_{eff} as a function of V , **a** for different χ , **b** for different x , **c** for different n (setting $q = 1$)

first-order phase transition when $0 < x < 1$. By substituting Eq. (3.12) into Eq. (2.20), we obtain

$$P_{\text{eff}} = \chi \frac{4(n-2)[f_1(x)f_6(x) - f_4(x)f_3(x)]}{(2n-3)r_c f_3(x)r_{cc}} - \frac{f_1(x)f_6(x) - f_4(x)f_3(x)}{r_c^2 f_3(x)} + \frac{q^2(f_5(x)f_3(x) - f_2(x)f_6(x))}{r_c^{2n-2} f_3(x)}, \quad (3.13)$$

The $P_{\text{eff}} - V$ curve for different χ , x , and n can be plotted from Eqs. (2.13) and (3.13) in Fig. 4.

The values of V_2 and V_1 for different effective temperatures T_{eff} (i.e., different values of χ) can be found using Eqs. (2.13) and (3.7). The red dots in the Fig. 4a indicate the boundary point of the coexistence region, and the intervals between the parallel horizontal coordinates of the two red dots represent the two-phase coexistence region. Figure 4b shows the behavior of effective pressure P_{eff} as a function of thermodynamic volume V under fixed spacetime dimension n and effective critical temperatures T_{eff}^c for the occurrence of the phase transition in HDTNS. By examining Fig. 4b, from the position ratio x of the two horizons, it is observed that the behavior of the effective pressure P_{eff} is different in different thermodynamic volume ranges, keeping the thermodynamic volume V constant. In the small (large) thermodynamic volume range, the effective pressure P_{eff} during the phase transition increases (decreases) with an increase in the position ratio x of the two horizons in the case of fixed V . Figure 4c shows that for the same thermodynamic volume V and position ratio x of the two horizons, the effective pressure P_{eff} increases with increasing spacetime dimension n .

The Gibbs free energy in HDTNS spacetime can be expressed as follows:

$$G(r_c, x) = M - T_{\text{eff}} S + P_{\text{eff}} V. \quad (3.14)$$

The $G_{T_{\text{eff}}} - P_{\text{eff}}$ curves for different χ are plotted in Fig. 5.

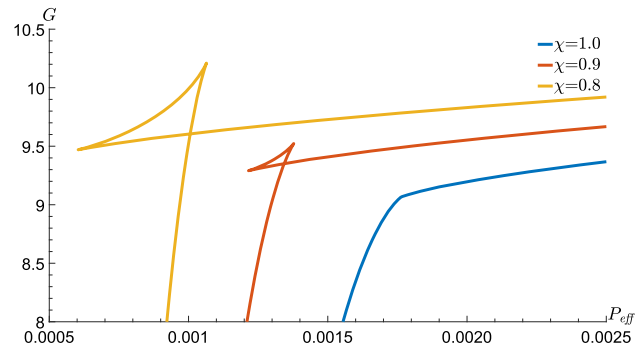


Fig. 5 The behavior of Gibbs free energy $G_{T_{\text{eff}}}$ as a function of the effective pressure P_{eff} given fixed $x = 0.4, n = 3$ for different χ (setting $q = 1$)

Comparing Fig. 4a with Fig. 5, when $\chi = 0.9$, that is, the effective temperature $T_{\text{eff}} < T_{\text{eff}}^c$, it is found that the $G_{T_{\text{eff}}} - P_{\text{eff}}$ curve contains an intersection, which is similar to that of the van der Waals system and the Ads black hole. The first-order phase transition occurs at the intersection of the isothermal $G_{T_{\text{eff}}} - P_{\text{eff}}$ curve in HDTNS spacetime according to the Gibbs free energy criterion at isothermal and isobaric conditions. When $\chi = 1$, the isothermal $G_{T_{\text{eff}}} - P_{\text{eff}}$ curve varies continuously with a single value, indicating that the HDTNS spacetime is in a single state. This state corresponds to the vapor phase of the VdW system.

To ensure that the thermodynamic system meets the requirements of equilibrium stability, the isothermal $P_{\text{eff}} - V$ curve cannot have negative pressure, and therefore the lowest temperature meets the requirements of

$$\left(\frac{\partial P_{\text{eff}}}{\partial V} \right)_{T_{\text{eff}}} = \left(\frac{\partial P_{\text{eff}}}{\partial r_c} \right)_{T_{\text{eff}}} \left(\frac{\partial r_c}{\partial V} \right)_{T_{\text{eff}}} = 0, \quad P_{\text{eff}}(V, T_{\text{eff}}) = 0. \quad (3.15)$$

From Eq. (3.12), we obtain

$$\frac{q^2}{r_{cmin}^{2n-4}} = \frac{f_1(x)f_6(x) - f_4(x)f_3(x)}{(2n-3)(f_5(x)f_3(x) - f_2(x)f_6(x))}. \quad (3.16)$$

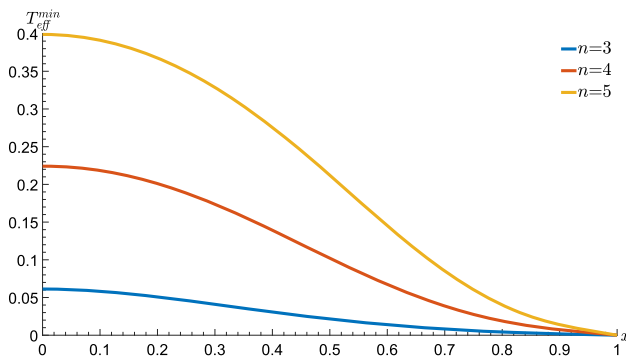


Fig. 6 The behavior of the lowest effective temperature T_{eff}^{\min} as a function of x for different n

The minimum temperature T_{eff}^{\min} of the spacetime satisfies

$$T_{\text{eff}}^{\min} = \frac{2(n-2)(f_1(x)f_6(x) - f_4(x)f_3(x))}{(2n-3)f_6(x)} \times \left(\frac{f_1(x)f_6(x) - f_4(x)f_3(x)}{(2n-3)q^2(f_5(x)f_3(x) - f_2(x)f_6(x))} \right)^{1/(2n-4)}. \quad (3.17)$$

The ratio of the minimum effective temperature T_{eff}^{\min} to the critical temperature T_{eff}^c of the spacetime

$$\frac{T_{\text{eff}}^{\min}}{T_{\text{eff}}^c} = \frac{(n-1)^{1/(2n-4)}}{2}, \quad (3.18)$$

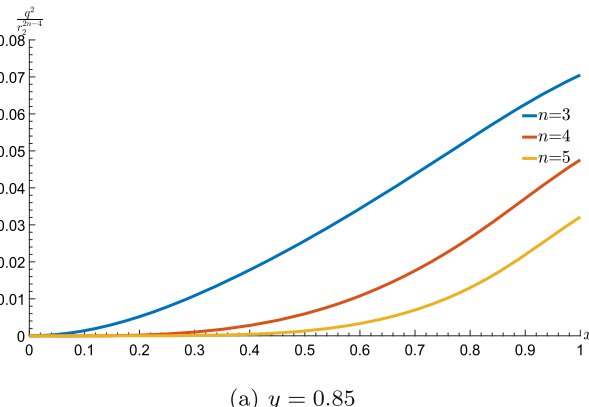
is independent of the ratio x of the positions of the two horizons, and is only related to the dimension n of the spacetime. The $T_{\text{eff}}^{\min} - x$ curve is plotted in Fig. 4 for different spacetime dimensions n . The behavior of T_{eff}^{\min} for a fixed x also increases with increasing n , which is consistent with Fig. 2b (Fig. 6).

The $\frac{q^2}{r_2^{2n-4}} - x$ and $\frac{q^2}{r_2^{2n-4}} - y$ curves for different n are plotted in Fig. 7 from Eq. (3.7). Figure 7 displays the correlation between the potential at the horizon and the spacetime

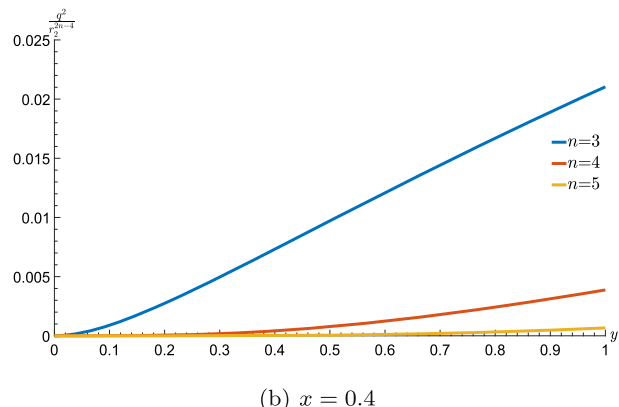
dimension n during a phase transition. Additionally, Fig. 7a depicts the behavior of the potential at the transition point as a function of the ratio x , which represents the black hole horizon position to the cosmological horizon position, for a given ratio y of the cosmological (or the black hole) horizon position of the two-phase coexistence regions. Furthermore, the potential at the boundary of the coexistence region decreases as the spacetime dimension n increases. Figure 7b illustrates the behavior of the potential at the phase transition point as a function of the ratio y , which represents the cosmological (or black hole) horizon position of the two-phase coexistence regions in spacetime, for a given ratio x of the black hole horizon position to the cosmological horizon position. It is evident from Eqs. (3.7) and (3.10) that the phase transition of the HDNTS spacetime depends on the cosmological (or black hole) horizon potential for a given effective temperature T_{eff} (i.e., χ is fixed), rather than that between a large black hole and a small black hole. The potential $\varphi_1 = \frac{q}{r_1^{2n-2}}$ at phase 1 with a small cosmological horizon radius is larger than the potential $\varphi_2 = \frac{q}{r_2^{2n-2}}$ at phase 2 with a large cosmological horizon radius, i.e. $\varphi_1 > \varphi_2$. In fact, for the given effective temperature T_{eff} , the HDTNS spacetime will be in a two-phase coexistence state if the corresponding potential satisfies $\varphi_1 \geq \varphi \geq \varphi_2$, while it will be in a single-phase state if the potential satisfies $\varphi > \varphi_1$ or $\varphi < \varphi_2$. Therefore, the HDTNS spacetime with the potential satisfied by $\varphi > \varphi_1$ or $\varphi < \varphi_2$ corresponds to the liquid or gas phase of the vdW system, respectively, and the HDTNS spacetime with the potential in the interval of $\varphi_1 \geq \varphi \geq \varphi_2$ corresponds to the gas–liquid coexistence region.

4 Two-phase equilibrium coexistence curve

In the two-phase coexistence region of a thermodynamic system, the Gibbs free energies must be equal. If pressure and



(a) $y = 0.85$



(b) $x = 0.4$

Fig. 7 The behavior of $\frac{q^2}{r_2^{2n-4}}$ as a function of x and y for different n , respectively

temperature are altered during two-phase coexistence, the Gibbs free energy of both phases must change by the same amount, i.e. $dG^1 = dG^2$. However, the Gibbs free energy of the two phases is not yet fully known for ordinary thermodynamic systems. To gain a better understanding of the two-phase coexistence region, the slope of the $P - T$ curve at the boundary of the two-phase coexistence, i.e. the Clapeyron equation, is provided.

$$\frac{dP}{dT} = \frac{L}{T(V_2 - V_1)}, \quad (4.1)$$

Here, $L = T(S_2 - S_1)$ represents the latent heat of the phase transition, and V_1 and V_2 stand for the volume of the system in phase 1 and phase 2, respectively. The Clapeyron equation agrees well with the experimental results for ordinary thermodynamic systems, providing direct verification of thermodynamic correctness. For the HDTNS spacetime thermodynamic system, by substituting Eq. (3.7) into Eqs. (3.6) and (3.5), we obtain the following.

When $n = 3$,

$$T_{\text{eff}}^0 = \frac{(f_1(x)f_6(x) - f_4(x)f_3(x))4y(1+y)}{qf_6(x)(1+4y+y^2)}$$

$$F_1(y) = \frac{(3+4y+3y^2)}{(3+12y+30y^2+60y^3+70y^4+60y^5+30y^6+12y^7+3y^8)}.$$

$$\times \left(\frac{f_1(x)f_6(x) - f_4(x)f_3(x)}{(f_5(x)f_3(x) - f_2(x)f_6(x))(1+4y+y^2)} \right)^{1/2}, \quad (4.2A)$$

$$P_{\text{eff}}^0 = \frac{3y^2(f_1(x)f_6(x) - f_4(x)f_3(x))^2}{f_3(x)q^2(f_5(x)f_3(x) - f_2(x)f_6(x))(1+4y+y^2)^2}. \quad (4.3A)$$

When $n = 4$,

$$T_{\text{eff}}^0 = \frac{3(f_1(x)f_6(x) - f_4(x)f_3(x))y(1+y)^3}{q^{1/2}f_6(x)(1+3y+7y^2+3y^3+y^4)} \times \left(\frac{(f_1(x)f_6(x) - f_4(x)f_3(x))}{(f_5(x)f_3(x) - f_2(x)f_6(x))} \right)^{1/4} \times \frac{1}{(1+3y+7y^2+3y^3+y^4)}, \quad (4.2B)$$

$$P_{\text{eff}}^0 = \frac{2y^2(f_1(x)f_6(x) - f_4(x)f_3(x))(1+3y+y^2)}{qf_3(x)(1+3y+7y^2+3y^3+y^4)}$$

$$\times \left(\frac{(f_1(x)f_6(x) - f_4(x)f_3(x))}{(f_5(x)f_3(x) - f_2(x)f_6(x))} \right)^{1/2} \times \frac{1}{(1+3y+7y^2+3y^3+y^4)}. \quad (4.3B)$$

When $n = 5$,

$$T_{\text{eff}}^0 = \frac{(f_1(x)f_6(x) - f_4(x)f_3(x))}{f_6(x)(1-y)} \times \left(\frac{(f_1(x)f_6(x) - f_4(x)f_3(x))}{q^2(f_5(x)f_3(x) - f_2(x)f_6(x))} F_1(y) \right)^{1/6} \times \left[(1-y^2) - F_1(y)(1-y^{2n-2}) \right], \quad (4.2C)$$

$$P_{\text{eff}}^0 = \frac{y^2(f_1(x)f_6(x) - f_4(x)f_3(x))}{f_3(x)} \times \left(\frac{(f_1(x)f_6(x) - f_4(x)f_3(x))F_1(y)}{q^2(f_5(x)f_3(x) - f_2(x)f_6(x))} F_1(y) \right)^{1/3} \times \left[\frac{(1-y^2) - F_1(y)(1-y^{2n-2})}{y(1-y)} - 1 + y^6 F_1(y) \right], \quad (4.3C)$$

with

The slope of the two-phase equilibrium $P_{\text{eff}}^0 - T_{\text{eff}}^0$ curve from Eqs. (4.2A) and (4.2B) for HDTNS satisfies the following.

When $n = 3$,

$$\frac{dP_{\text{eff}}^0}{dT_{\text{eff}}^0} = \frac{3f_6(x)}{4qf_3(x)} \left(\frac{(f_1(x)f_6(x) - f_4(x)f_3(x))}{(f_5(x)f_3(x) - f_2(x)f_6(x))} \right)^{1/2} \frac{F'_{1A}(y)}{F'_{2A}(y)}, \quad (4.4A)$$

with

$$F_{1A}(y) = \frac{y^2}{(1+4y+y^2)^2}, \quad F_{2A}(y) = \frac{y(1+y)}{(1+4y+y^2)^{3/2}}, \quad (4.5A)$$

$$F'_{1A}(y) = \frac{dF_{1A}(y)}{dy}, \quad F'_{2A}(y) = \frac{dF_{2A}(y)}{dy}.$$

When $n = 4$,

$$\frac{dP_{\text{eff}}^0}{dT_{\text{eff}}^0} = \frac{f_6(x)}{q^{1/2}f_3(x)} \left(\frac{(f_1(x)f_6(x) - f_4(x)f_3(x))}{(f_5(x)f_3(x) - f_2(x)f_6(x))} \right)^{1/4} \frac{F'_{1B}(y)}{F'_{2B}(y)}, \quad (4.4B)$$

with

$$\begin{aligned} F_{1B}(y) &= \frac{y^2(1+3y+y^2)}{(1+3y+7y^2+3y^3+y^4)} \\ &\times \left(\frac{1}{(1+3y+7y^2+3y^3+y^4)} \right)^{1/2}, \\ F_{2B}(y) &= \frac{y(1+y)^3}{(1+3y+7y^2+3y^3+y^4)} \\ &\times \left(\frac{1}{(1+3y+7y^2+3y^3+y^4)} \right)^{1/4}. \end{aligned} \quad (4.5B)$$

When $n = 5$,

$$\frac{dP_{\text{eff}}^0}{dT_{\text{eff}}^0} = \frac{f_6(x)}{f_3(x)} \left(\frac{(f_1(x)f_6(x) - f_4(x)f_3(x))}{q^2(f_5(x)f_3(x) - f_2(x)f_6(x))} \right)^{1/6} \frac{F'_{1C}(y)}{F'_{2C}(y)}, \quad (4.4C)$$

with

$$\begin{aligned} F_{1C}(y) &= y^2 (F_1(y))^{1/3} \\ &\times \left[\frac{(1-y^2) - F_1(y)(1-y^{2n-2})}{y(1-y)} - 1 + y^6 F_1(y) \right], \\ F_{2C}(y) &= \frac{(F_1(y))^{1/6}}{(1-y)} [(1-y^2) - F_1(y)(1-y^{2n-2})]. \end{aligned} \quad (4.5C)$$

Equations (4.4A-C) represent the slope of the $P_{\text{eff}}^0 - T_{\text{eff}}^0$ curve when the two phases coexist in equilibrium.

The latent heat L of the phase transition of the HDTNS spacetime thermodynamic system can be obtained from Eqs. (4.1) and (4.4).

$$\begin{aligned} L &= \frac{4\pi(1+y)(1-y^3)q}{y^2f_3(x)} ((f_5(x)f_3(x) - f_2(x)f_6(x)) \\ &\times (f_1(x)f_6(x) - f_4(x)f_3(x)))^{1/2} \frac{F'_1(y)}{F'_2(y)}, \end{aligned} \quad (4.6A)$$

$$\begin{aligned} L &= \frac{V_3(1-y^4)}{4y^4f_3(x)} \frac{q^2(f_5(x)f_3(x) - f_2(x)f_6(x))^{1/2}(f_1(x)f_6(x) - f_4(x)f_3(x))^{1/2}}{1+y+y^2} \\ &\times (1+3y+7y^2+3y^3+y^4)^{3/4}(1+y)^3 \frac{F'_{1B}(y)}{F'_{2B}(y)}, \end{aligned} \quad (4.6B)$$

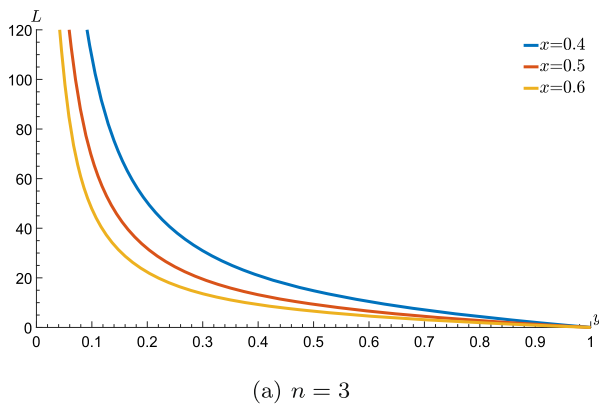
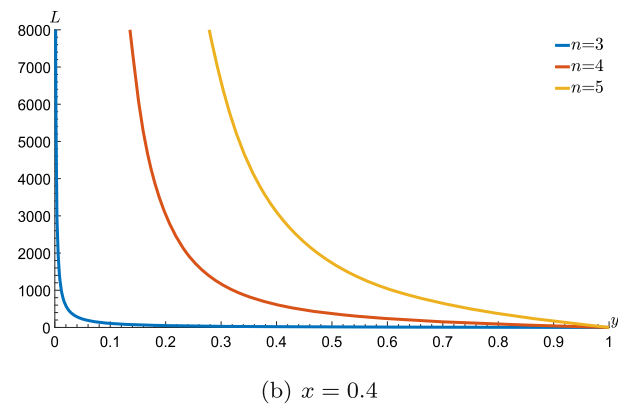
$$\begin{aligned} L &= \frac{qV_4(1-y^5)}{5y^5(F_1(y))^{2/3}(1-y)} \frac{F'_{1C}(y)}{F'_{2C}(y)} 0 \left[(1-y^2) - F_1(y)(1-y^{2n-2}) \right] \\ &\times \frac{(f_5(x)f_3(x) - f_2(x)f_6(x))^{1/2}(f_1(x)f_6(x) - f_4(x)f_3(x))^{1/2}}{f_3(x)}. \end{aligned} \quad (4.6C)$$

The latent heat of the phase transition can be expressed as a function of x and y by using Eq. (4.6) with q set to 1. The plotted $L - y$ curve is shown in Fig. 8.

Figure 8a shows that the latent heat L of a first-order phase transition in spacetime decreases as the ratio x of the positions of the two horizons increases for a fixed y , while keeping the spacetime dimensions n fixed. The data presented in Fig. 8b show that the latent heat L of the phase transition increases as the spacetime dimensions n increase, while keeping the ratio x of the positions of the two horizons fixed. Additionally, based on Fig. 8, the effect of the ratio x of the positions of the two horizons on the latent heat L of the phase transition for first-order phase transition in spacetime is less significant than that of spacetime dimensions n , provided that all other factors remain constant.

5 Conclusion

Black hole thermodynamics serve as a connection between general relativity, classical thermodynamics, and quantum mechanics. The topic is of significant interest due to its direct relation to various fields of physics, including gravity, statistics, and particle and field theory, in which black hole thermodynamics play a crucial role. Although the statistical description of the corresponding thermodynamic states of black holes remains unclear, the study of the thermodynamic properties of black holes and the critical phenomena remain of interest. This paper extends the study of black hole thermodynamic properties to the HDTNS spacetime and discusses the extended phase transition based on the effective thermodynamic quantities in HDTNS spacetime. The phase transition of HDTNS spacetime is analyzed by applying Maxwell's equal-area law, revealing similarities to the van der Waals system. The potential at the horizon depends on the horizon position, the potential charge, and the position ratio x between the two horizons, as given by Eq. (3.7), when the effective temperature T_{eff}^0 of spacetime is provided. It is

(a) $n = 3$ (b) $x = 0.4$ **Fig. 8** The behavior of L as a function of y for different x and n , respectively (setting $q = 1$)

important to note that this differs from the phase transition observed in AdS black holes [57, 58]. Figure 7 illustrates the relationship between the potential at the horizon and the position ratio x between two horizons, as well as the spacetime dimension n , when a phase transition occurs in spacetime. In the vdW system, the phase transition at a fixed temperature is primarily due to the interaction between molecules within the system. In HDTNS spacetime, however, the phase transition is mainly caused by the magnitude of the electric field experienced by the “molecules” of this system. For the system in the high potential state, where the “molecules” are arranged in an orderly manner under the influence of a strong electric field, the system is in an ordered phase. Conversely, in the low potential phase, where the “molecules” are arranged in a disorderly manner under the influence of a weak electric field, the system is in a disordered phase. The molecules affected by thermal fluctuations and electric fields are in the phase transition region between disorder and order, or order and disorder, when the system is in the two-phase coexistence state.

According to the discussion in Sect. 3, when the HDTNS spacetime has a temperature greater than its minimum effective temperature, T_{eff}^{\min} , its effective pressure, P_{eff} , is also greater than zero. This meets the requirement for the thermodynamic system to be in a stable equilibrium state. Therefore, we consider the sign in front of the $P_{\text{eff}} dV$ term in Eq. (2.12) to be a positive sign, which satisfies the first law of thermodynamics relative to HDTNS spacetime. This is different from the literature [62], where the $P_{\text{eff}} dV$ term in Eq. (5) is taken as a negative sign. Equation (3.18) demonstrates that the ratio between the minimum effective temperature T_{eff}^{\min} and the critical effective temperature T_{eff}^c of the HDTNS spacetime is independent of the ratio x between the two horizons. This conclusion is consistent with the findings for AdS black holes [63, 64].

This work examines the thermodynamic properties of HDTNS spacetime and investigates the effect of spacetime dimensions n and the ratio x between two horizons on these properties. The microstates of the internal “molecules” during the phase transition of spacetime are useful for exploring the microstructure of dS spacetime in depth. The study of the microstructure of black holes is particularly important for understanding their fundamental properties in gravity and for the establishment of quantum gravity.

Acknowledgements We would like to thank Prof. Ren Zhao and Meng-Sen Ma for their indispensable discussions and comments. This work was supported by the Natural Science Foundation of China (Grant no. 12375050, Grant no. 11705106, Grant no. 12075143), the Scientific Innovation Foundation of the Higher Education Institutions of Shanxi Province (Grant nos. 2023L269), the Science Foundation of Shanxi Datong University (2022Q1, 2020Q2), the Natural Science Foundation of Shanxi Province (Grant no. 202203021221209, Grant no. 202303021211180), the Teaching Reform Project of Shanxi Datong University (XJG2022234) and the Program of State Key Laboratory of Quantum Optics and Quantum Optics Devices (KF202403).

Data availability statement This manuscript has associated code/software in a data repository. [Author’s comment: In our work, there is no experimental data, just has the numerical calculated data obtained from the theoretical analyze.]

Code availability statement This manuscript has associated data in a data repository. [Author’s comment: The code developed from the theoretical analyze and can be available from the corresponding author on reasonable request.]

Open Access This article is licensed under a Creative Commons Attribution 4.0 International License, which permits use, sharing, adaptation, distribution and reproduction in any medium or format, as long as you give appropriate credit to the original author(s) and the source, provide a link to the Creative Commons licence, and indicate if changes were made. The images or other third party material in this article are included in the article’s Creative Commons licence, unless indicated otherwise in a credit line to the material. If material is not included in the article’s Creative Commons licence and your intended use is not permitted by statutory regulation or exceeds the permitted use, you will need to obtain permission directly from the copyright holder. To view a copy of this licence, visit <http://creativecommons.org/licenses/by/4.0/>

References

- D. Kubiznak, R.B. Mann, P-V criticality of charged AdS black holes. *JHEP* **1207**, 033 (2012). [arXiv:1205.0559](https://arxiv.org/abs/1205.0559)
- D. Kubiznak, R. B. mann, M. Teo, Black hole chemistry: thermodynamics with Lambda. *Class. Quantum Gravity* **34**, 063001 (2017). [arXiv:1608.06147](https://arxiv.org/abs/1608.06147) [hep-th]
- S. Gunasekaran, D. Kubiznak, R.B. Mann, Extended phase space thermodynamics for charged and rotating black holes and Born-Infeld vacuum polarization. *JHEP* **2012**, 11 (2012). [arXiv:1208.6251](https://arxiv.org/abs/1208.6251)
- R.A. Hennigar, R.B. Mann, Superfluid black hole. *Phys. Rev. L* **118**, 021301 (2017)
- R.G. Cai, L.M. Cao, L. Li, R.Q. Yang, criticality in the extended phase space of Gauss–Bonnet black holes in AdS space. *JHEP* **9**, 1–22 (2013). [arXiv:1306.6233](https://arxiv.org/abs/1306.6233) [gr-qc]
- R.G. Cai, S.M. Ruan, S.J. Wang, R.Q. Yang, R.H. Peng, Complexity growth for AdS black holes. *JHEP* **1609**, 161 (2016). [arXiv:1606.08307](https://arxiv.org/abs/1606.08307)
- J.L. Zhang, R.G. Cai, H.W. Yu, Phase transition and thermodynamical geometry of Reissner–Nordstrom–AdS black holes in extended phase space. *Phys. Rev. D* **91**, 044028 (2015). [arXiv:1502.01428](https://arxiv.org/abs/1502.01428)
- J.L. Zhang, R.G. Cai, H.W. Yu, Phase transition and thermodynamical geometry for Schwarzschild AdS black hole in AdS spacetime. *JHEP* **02**, 143 (2015). [arXiv:1409.5305](https://arxiv.org/abs/1409.5305)
- X.Q. Li, H.P. Yan, L.L. Xing, S.W. Zhou, Critical behavior of AdS black holes surrounded by dark fluid with Chaplygin-like equation of state. *Phys. Rev. D* **107**, 104055 (2023). [arXiv:2305.03028](https://arxiv.org/abs/2305.03028) [gr-qc]
- M. Estrada, R. Aros, Thermodynamic extended phase space and criticality of black holes at Pure Lovelock gravity. *Eur. Phys. J. C* **80**, 395 (2020). [arXiv:1909.07280v3](https://arxiv.org/abs/1909.07280v3)
- S.W. Wei, Y.X. Liu, Insight into the microscopic structure of an AdS black hole from a thermodynamical phase transition. *Phys. Rev. Lett.* **115**, 111302 (2015). [arXiv:1502.00386](https://arxiv.org/abs/1502.00386) [gr-qc]
- S.J. Yang, J. Tao, B.R. Mu, A.Y. He, Lyapunov exponents and phase transitions of Born–Infeld AdS black holes, CTP-SCU/2023005. [arXiv:2304.01877](https://arxiv.org/abs/2304.01877) [gr-qc]
- S.H. Hendi, Kh. Jafarzade, Critical behavior of charged AdS black holes surrounded by quintessence via an alternative phase space. *Phys. Rev. D* **103**, 104011 (2021). [arXiv:2012.13271](https://arxiv.org/abs/2012.13271)
- M. Momennia, S.H. Hendi, Critical phenomena and reentrant phase transition of asymptotically Reissner–Nordstrom black holes. *Phys. Lett. B* **822**, 136692 (2021). [arXiv:2101.12039](https://arxiv.org/abs/2101.12039) [gr-qc]
- S.H. Hendi, S. Hajkhahili, M. Jamil, M. Momennia, Stability and phase transition of rotating Kaluza–Klein black holes. *Eur. Phys. J. C* **81**, 1112 (2021). [arXiv:2111.10117](https://arxiv.org/abs/2111.10117) [gr-qc]
- N.C. Bai, A.Y. He, J. Tao, Microstructure of charged AdS black hole with minimal length effects, CTP-SCU/2022005. [arXiv:2204.13044](https://arxiv.org/abs/2204.13044) [gr-qc]
- A. Sood, A. Kumar, J.K. Singh, S.G. Ghosh, Thermodynamic stability and P-V criticality of nonsingular-AdS black holes endowed with clouds of strings. *Eur. Phys. J. C* **82**, 227 (2022). [arXiv:2204.05996](https://arxiv.org/abs/2204.05996) [gr-qc]
- Y.Z. Du, H.F. Li, F. Liu, R. Zhao, L.C. Zhang, Phase transition of non-linear charged anti-de Sitter black holes. *Chin. Phys. C* **45**(11), 115103 (2021). [arXiv:2112.10403](https://arxiv.org/abs/2112.10403) [hep-th]
- Z.M. Xu, B. Wu, W.L. Yang, Ruppeiner thermodynamic geometry for the Schwarzschild-AdS black hole. *Phys. Rev. D* **101**, 024018 (2020). [arXiv:1910.12182](https://arxiv.org/abs/1910.12182)
- G. R. Li, G. P. Li, S. Guo, Phase transition grade and microstructure of AdS black holes in massive gravity. *Class. Quantum Gravity* **39**(19), 195011 (2022). [arXiv:2304.00842](https://arxiv.org/abs/2304.00842) [gr-qc]
- D. Kubiznak, F. Simovic, Thermodynamics of horizons: de Sitter black holes and reentrant phase transitions. *Class. Quantum Grav.* **33**(24), 245001 (2016). [arXiv:1507.08630](https://arxiv.org/abs/1507.08630) [hep-th]
- R. Zhou, S.W. Wei, Novel equal area law and analytical charge-electric potential criticality for charged anti-de Sitter black holes. *Phys. Lett. B* **792**, 406 (2019)
- H. Ranjbari, M. Sadeghi, M. Ghanaatian, Gh. Forozani, Critical behavior of AdS Gauss–Bonnet massive black holes in the presence of external string cloud. *Eur. Phys. J. C* **80**, 17 (2020)
- M.M. Stetsko, Static spherically symmetric Einstein–Yang–Mills-dilaton black hole and its thermodynamics. *Phys. Rev. D* **101**, 124017 (2020). [arXiv:2005.13447](https://arxiv.org/abs/2005.13447) [hep-th]
- X.Y. Guo, H.F. Li, L.C. Zhang, R. Zhao, Continuous phase transition and microstructure of charged AdS black hole with quintessence. *Eur. Phys. J. C* **80**, 168 (2020). [arXiv:1911.09902](https://arxiv.org/abs/1911.09902) [gr-qc]
- R.A. Konoplya, A. Zhidenko, (In)stability of black holes in the 4D Einstein–Gauss–Bonnet and Einstein–Lovelock gravities. *Phys. Dark Universe* **30**, 100697 (2020). [arXiv:2003.12492](https://arxiv.org/abs/2003.12492)
- H.F. Li, X.Y. Guo, H.H. Zhao, R. Zhao, Maxwell’s equal area law for black holes in power Maxwell invariant. *Gen. Relativ. Gravit.* **49**(8), 111 (2017). [arXiv:1610.05428](https://arxiv.org/abs/1610.05428)
- J.M. Maldacena, The large N limit of superconformal field theories and super gravity. *Int. J. Theor. Phys.* **38**, 1113–1133 (1999)
- G. Policastro, D.T. Son, A.O. Starinets, From AdS/CFT correspondence to hydrodynamics. *J. High Energy Phys.* **2002**, 043 (2002)
- A. Strominger, The dS/CFT correspondence. *J. High. Ener. Phys.* **0110**, 034 (2001)
- N. Altamirano, D. Kubiznak, R.B. Mann, Z. Sherkatghanad, Kerr-AdS analogue of thruple point and solid/liquid/gas phase transition. *Class. Quantum Gravity* **31**, 042001 (2014). [arXiv:1308.2672](https://arxiv.org/abs/1308.2672)
- N. Altamirano, D. Kubiznak, R.B. Mann, Reentrant phase transitions in rotating anti-de Sitter black holes. *Phys. Rev. D* **88**, 101502 (2013). [arXiv:1306.5756](https://arxiv.org/abs/1306.5756)
- C.V. Johnson, Holographic heat engines. *Class. Quantum Gravity* **31**, 205002 (2014). [arXiv:1404.5982](https://arxiv.org/abs/1404.5982)
- A.G. Riess, A.V. Filippenko et al., Observational evidence from supernovae for an accelerating universe and a cosmological constant. *Astr. J.* **116**, 1009–1038 (1998). [arXiv:astro-ph/9805201v1](https://arxiv.org/abs/astro-ph/9805201v1)
- S. Perlmutter, G. Aldering et al., Measurements of Omega and Lambda from 42 high-redshift supernovae. *Astron. J.* **517**, 565–586 (1999). [arXiv:astro-ph/9812133](https://arxiv.org/abs/astro-ph/9812133)
- A.G. Riess, P.E. Nugent et al., The farthest known supernova: support for an accelerating universe and a glimpse of the epoch of deceleration. *Astron. J.* **560**, 49–71 (2001). [arXiv:astro-ph/0104455](https://arxiv.org/abs/astro-ph/0104455)
- Y. Sekiwa, Thermodynamics of de Sitter black holes: thermal cosmological constant. *Phys. Rev. D* **73**, 084009 (2006). [arXiv:hep-th/0602269](https://arxiv.org/abs/hep-th/0602269)
- B.P. Dolan, D. Kastor, D. Kubiznak, R.B. Mann, J. Traschen, Thermodynamic volumes and isoperimetric inequalities for de Sitter black holes. *Phys. Rev. D* **87**, 104017 (2013). [arXiv:1301.5926](https://arxiv.org/abs/1301.5926)
- S. Mbarek, R.B. Mann, Reverse Hawking–Page phase transition in de Sitter black holes. *JHEP* **02**, 103 (2019). [arXiv:1808.03349](https://arxiv.org/abs/1808.03349) [hep-th]
- H. Ranjbari, M. Sadeghi, M. Ghanaatian, Gh. Forozani, Critical behavior of AdS Gauss–Bonnet massive black holes in the presence of external string cloud. *Eur. Phys. J. C* **80**, 17 (2020). [arXiv:1911.10803](https://arxiv.org/abs/1911.10803)
- D. Kubiznak, F. Simovic, Thermodynamics of horizons: de Sitter black holes and reentrant phase transitions. *Class. Quantum Gravity* **33**, 245001 (2016). [arXiv:1507.08630](https://arxiv.org/abs/1507.08630)

42. R.G. Cai, Cardy–Verlinde formula and asymptotically de Sitter spaces. *Phys. Lett. B* **525**, 331 (2002). [arXiv:hep-th/0111093](https://arxiv.org/abs/hep-th/0111093)
43. R.G. Cai, Cardy–Verlinde formula and thermodynamics of black holes in de Sitter spaces. *Nucl. Phys. B* **628**, 375 (2002). [arXiv:hep-th/0112253](https://arxiv.org/abs/hep-th/0112253)
44. M. Urano, A. Tomimatsu, H. Saida, Mechanical first law of black hole spacetimes with cosmological constant and its application to Schwarzschild–de Sitter spacetime. *Class. Quantum Gravity* **25**, 105010 (2009). [arXiv:0903.4230](https://arxiv.org/abs/0903.4230)
45. M.S. Ma, H.H. Zhao, L.C. Zhang, R. Zhao, Existence condition and phase transition of Reissner–Nordstrom–de Sitter black hole. *Int. J. Mod. Phys. A* **29**, 1450050 (2014). [arXiv:1312.0731](https://arxiv.org/abs/1312.0731)
46. M.S. Ma, L.C. Zhang, H.H. Zhao, R. Zhao, Phase transition of the higher dimensional charged Gauss–Bonnet black hole in de Sitter spacetime. *Adv. High Energy Phys.* **2015**, 134815 (2015). [arXiv:1410.5950](https://arxiv.org/abs/1410.5950)
47. H.W. Braden, J.D. Brown, B.F. Whiting, J.W. York, Charged black hole in a grand canonical ensemble. *Phys. Rev. D* **42**, 3376 (1990)
48. S. Carlip, S. Vaidya, Phase transitions and critical behavior for charged black holes. *Class. Quantum Gravity* **20**, 3827–3838 (2003)
49. S.H. Hendi, M. Momennia, Thermodynamic instability of topological black holes with nonlinear source. *Eur. Phys. J. C* **75**, 54 (2015). [arXiv:1501.04863](https://arxiv.org/abs/1501.04863)
50. S.H. Hendi, R. Naderi, Geometrothermodynamics of black holes in Lovelock gravity with a nonlinear electrodynamics. *Phys. Rev. D* **91**, 024007 (2015). [arXiv:1510.06269v1](https://arxiv.org/abs/1510.06269v1)
51. S.H. Hendi, S. Panahiyan, M. Momennia, Extended phase space of AdS black holes in Einstein–Gauss–Bonnet gravity with a quadratic nonlinear electrodynamics. *Int. J. Mod. Phys. D* **25**, 1650063 (2016). [arXiv:1503.03340v2](https://arxiv.org/abs/1503.03340v2) [gr-qc]
52. S.N. Sajadi, N. Riazi, S.H. Hendi, Dynamical and thermal stabilities of nonlinearly charged AdS black holes. *Eur. Phys. J. C* **79**, 775 (2019). [arXiv:2003.13472](https://arxiv.org/abs/2003.13472)
53. S.H. Hendi, A. Dehghani, Criticality and extended phase space thermodynamics of AdS black holes in higher curvature massive gravity. *Eur. Phys. J. C* **79**, 227 (2019). [arXiv:1811.01018](https://arxiv.org/abs/1811.01018)
54. S.H. Hendi, M. Momennia, Thermodynamic description and quasi-normal modes of AdS black holes in Born–Infeld massive gravity with a non-abelian hair. *JHEP* **10**, 207 (2019)
55. A. Ali, K. Saifullah, Magnetized topological black holes of dimensionally continued gravity. *Phys. Rev. D* **99**, 124052 (2019)
56. X.X. Zeng, L.F. Li, Van der Waals phase transition in the framework of holography. *Phys. Lett. B* **764**, 100 (2017)
57. X. Y. Guo, H. F. Li, R. Zhao, Maxwell’s equal-area law with several pairs of conjugate variables for RN-AdS black holes. *Eur. Phys. J. P* **134**, 277 (2019)
58. H.F. Li, H.H. Zhao, L.C. Zhang, R. Zhao, Clapeyron equation and phase equilibrium properties in higher dimensional charged topological dilaton AdS black holes with a nonlinear source. *Eur. Phys. J. C* **77**, 295 (2017)
59. G.T. Horowitz, A. Strominger, Counting states of near-extremal black holes. *Phys. Rev. Lett.* **77**, 2368 (1996). [arXiv:hep-th/9602051v2](https://arxiv.org/abs/hep-th/9602051v2)
60. X.Y. Guo, H.F. Li, L.C. Zhang, R. Zhao, Microstructure and continuous phase transition of RN-AdS black hole. *Phys. Rev. D* **100**, 064036 (2019). [arXiv:1901.04703](https://arxiv.org/abs/1901.04703) [gr-qc]
61. H.H. Zhao, L.C. Zhang, Y. Gao, F. Liu, Entropic force between two horizons of dilaton black holes with a power-Maxwell field. *Chin. Phys. C* **45**, 4 (2021). [arXiv:2101.10051](https://arxiv.org/abs/2101.10051)
62. Y.Z. Du, R. Zhao, L.C. Zhang, Continuous phase transition of higher-dimensional de-Sitter spacetime with non-linear source. *Eur. Phys. J. C* **82**, 370 (2022). [arXiv:2104.10309](https://arxiv.org/abs/2104.10309)
63. J. Barrientos, J. Mena, Joule–Thomson expansion of AdS black holes in quasitopological electromagnetism. *Phys. Rev. D* **106**, 044064 (2022). [arXiv:2206.06018v2](https://arxiv.org/abs/2206.06018v2) [gr-qc]
64. S.I. Kruglov, Magnetically charged AdS black holes and Joule–Thomson expansion. *Gravity Cosmol* **29**(1), 57–61 (2023). [arXiv:2304.02121v1](https://arxiv.org/abs/2304.02121v1) [physics.gen-ph]